Optical Engineering

OpticalEngineering.SPIEDigitalLibrary.org

Combined line-of-sight error and angular position to generate feedforward control for a charge-coupled device–based tracking loop

Tao Tang
Huaxiang Cai
Yongmei Huang
Ge Ren

SPIE.

Combined line-of-sight error and angular position to generate feedforward control for a charge-coupled device–based tracking loop

Tao Tang,[a,b,*] Huaxiang Cai,[a,b] Yongmei Huang,[a,b] and Ge Ren[a,b]
[a]Chinese Academy of Sciences, Key Laboratory of Optical Engineering, Chengdu 610209, China
[b]Chinese Academy of Sciences, The Institute of Optics and Electronics, Chengdu 610209, China

Abstract. A feedforward control based on data fusion is proposed to enhance closed-loop performance. The target trajectory as the observed value of a Kalman filter is recovered by synthesizing line-of-sight error and angular position from the encoder. A Kalman filter based on a Singer acceleration model is employed to estimate the target velocity. In this control scheme, the control stability is influenced by the bandwidth of the Kalman filter and time misalignment. The transfer function of the Kalman filter in the frequency domain is built for analyzing the closed loop stability, which shows that the Kalman filter is the major factor that affects the control stability. The feedforward control proposed here is verified through simulations and experiments. [DOI: 10.1117/1.OE.54.10.105107]

Keywords: feedforward control; charge-coupled device based; time delay; line-of-sight error; Kalman filter.

Paper 150567 received May 2, 2015; accepted for publication Sep. 9, 2015; published online Oct. 15, 2015.

1 Introduction

Two-axis (azimuth and elevation) gimbals with a charge-coupled device (CCD)-based control system can be used for monitoring and positioning as well as tracking an interesting target.[1–3] The basic mechanism and configuration is a two-axis gimbal equipped mainly with motor, encoder, CCD, and other components.[2,3] Unlike the previous control problem, the tracker of CCD cannot provide the target trajectory or the target velocity, but only line-of-sight (LOS) error. A direct feedback loop is usually utilized to control LOS. High control bandwidth (BW) facilitates good closed loop performance. However, the time delay is the major reason to restrict the BW in a CCD-based tracking loop. In general, there are three factors causing the time delay to the closed loop system: exposure time of the CCD, image process time, and transmit time. The time delay cannot be cut to zero, which results in an ineffectiveness of a high BW. A feedforward control, such as a rate-aided control, is introduced into a CCD-based tracking system to reduce the LOS error.[4,5] The target trajectory either can be recovered through sensor fusion, including a rangefinder, the CCD, encoder, and rate sensor, or can be given. Experiments verify rate the feedforward control to be effective for improving the tracking performance, especially for a maneuvering target tracking. Motivated by pervious research,[6,7] an improved feedforward control is proposed in this paper. This method only combines the CCD and encoder for data fusion to recover the target trajectory as an observed value of the Kalman filter, which can produce the target velocity to implement the feedforward control. The previous researches usually focused on how to optimize the Kalman filter or how to make precise models for better estimation of the target rate.[8–10] However, if the target trajectory is unknown, it is necessary to consider the closed loop stability when a Kalman filter is used to estimate the target velocity. To analyze the closed loop stability, the transfer function of a Kalman filter in the frequency domain is built.

Section 2 presents a detailed introduction to a feedforward control, mainly describing the CCD-based control structure and the implementation of the feedforward control. Section 3 focuses on parameters' design, specifically in terms of the proportional-integral (PI) controller and the Kalman filter. Section 4 discusses and analyzes the system stability. Section 5 sets up experiments to verify this method. Concluding remarks are presented in Sec. 6.

2 Feedforward Control

A classical feedforward control is shown in Fig. 1, where $Q(s)$ is the feedforward controller, $C(s)$ is the position controller, and $P(s)$ is the control plant. The time delay $e^{-T_0 s}$ characterizes the CCD in the control system, although it may be rough.

The feedforward control not only has little influence on the closed loop stability, but also contributes a lot to the control performance. However, the tracking sensor cannot provide the target trajectory or target speed, but only an LOS error in a CCD-based servo control system. Considering $R = E + Y$, the equivalent control structure of Fig. 1 is depicted in Fig. 2.

This control structure in Fig. 2 is practical. The target trajectory can be recovered by combining the LOS error and the angular position of the gimbals. The sensitivity function is

$$S_{\mathrm{SF}} = \frac{1 - Q(s)P(s)e^{-T_1 s}}{1 + C(s)P(s)e^{-T_0 s} + Q(s)P(s)(e^{-T_0 s} - e^{-T_1 s})}. \quad (1)$$

The improvement of the feedforward control is mainly subject to $1 - e^{-T_0 s}$ if this feedforward controller $Q(s)$ is

*Address all correspondence to: Tao Tang, E-mail: prettang@gmail.com

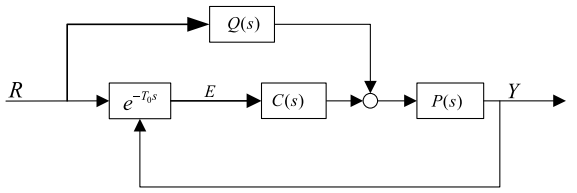

Fig. 1 classical feedforward control.

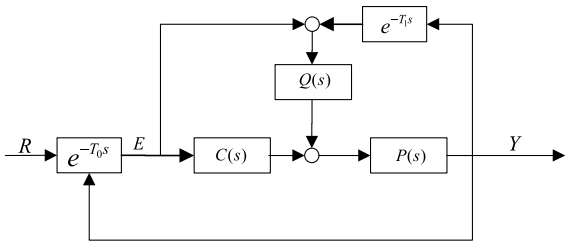

Fig. 2 An equivalent feedforward control.

designed to be the inverse $P(s)$. It is obvious that the term $1-e^{-T_1 s}$ is close to $T_1 s$ in low frequencies. In this situation, the smaller the time parameter is set, the more the feedforward control contributes to the closed-loop performance. However, it is impractical to implement $Q(s)=P^{-1}(s)$, because the term $P(s)$ includes not only the non-nominal part, but also the high-frequency characteristics.

$P(s)$ is depicted in Fig. 3, where $G(s)$ is the control plant and $C_v(s)$ is the velocity controller designed according to the classical control theorem. A tachometer providing the angular velocity of the gimbals usually has a high BW, resulting only in a minor influence on the closed-loop control system.

We can easily get the transfer function from O to V in Fig. 3:

$$P(s)=\frac{O}{V}=\frac{C_v(s)G(s)}{1+C_v(s)G(s)}\frac{1}{s}. \tag{2}$$

As a matter of fact, this term $C_v(s)G(s)/1+C_v(s)G(s)$ is very close to constant 1 in low frequencies because the velocity closed loop has a much higher BW than that of the position closed loop. Thus, $P(s)\approx 1/s$ is true to some extent. In this case, the feedforward controller can be described as

$$Q(s)=\frac{s}{1+T_f s}. \tag{3}$$

The phase lag term $1/1+T_f s$ indicates the main feature of a filter. It is impossible to obtain the velocity by directly differentiating the synthesizing signal $E+Y$, because noise can pollute the differential signal, resulting in ineffectiveness.

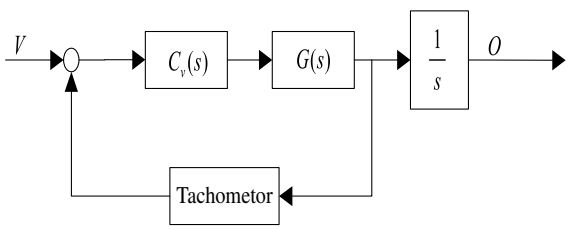

Fig. 3 The velocity closed-loop control.

The open-loop transfer function in Fig. 2 is given by Eq. (4):

$$S_{\text{open}}=\frac{Q(s)P(s)+C(s)P(s)}{1-Q(s)P(s)e^{-T_1 s}}e^{-T_0 s}. \tag{4}$$

From Eqs. (1) and (4), the difference between the two parameters and the filter $Q(s)$ may affect the stability or even lead to control instability.

3 Parameters Design

The sampling frequency of the CCD is 50 Hz. The time delay T_0 is 0.06 s, which is about three times more than the sampling interval of 0.02 s. The position open-loop transfer function without a feedforward control is in Eq. (5):

$$e^{-T_0 s}C(s)P(s)\approx\frac{K_p(K_I s+1)}{s}\frac{e^{-T_0 s}}{s}. \tag{5}$$

For the feedback system to be robust, a gain margin larger than 6 dB and a phase margin larger than 35 deg is usually specified.[11] Given w_c is the crossover frequency of the open-loop transfer function, according to the definition of the phase margin, we have

$$\begin{cases}\arctan(K_I w_c)-T_0 w_c=\frac{\pi}{4}\\ K_p\sqrt{K_I^2 w_c^2+1}=w_c^2\end{cases}. \tag{6}$$

Combining the two equations to remove the integral parameter K_I yields Eq. (9):

$$K_p=w^2\cos\left(T_0 w_c+\frac{\pi}{4}\right). \tag{7}$$

Let $\partial K_p/\partial w=0$, then the maximum gain can be obtained and $w_c T_0\approx 0.5275$ is resolved. Substituting this into Eqs. (6) and (7), the PI controller parameters can be resolved as $K_p=0.0709/T_0^2=19.71$ and $K_I=7.188\ T_0=0.43$.

Approximating $e^{T_1 s}\approx 1/1+T_1 s$ and $Q(s)P(s)\approx 1/1+T_f s$, where $1/1+T_f s$ is referred to as the characteristics of the Kalman filter, Eq. (4) can be rewritten into Eq. (8):

$$\begin{aligned}&\arg[S_{\text{open}}(s)|_{s=jw_c'}]\\&=\arg\left[\frac{[K_p(K_I s+1)(T_f s+1)+1](T_0 s+1)}{T_f T_0 s+T_f+T_0}\frac{e^{-T_0 s}}{s^3}|_{s=jw_c'}\right]\\&\approx\arctan(T_0 w_c')+\arctan(K_I w_c')+\arctan(T_f w_c')\\&\quad-T_0 w_c'-\arctan\left(\frac{T_f T_0 w_c'}{T_f+T_0}\right)-\frac{3}{2}\pi.\end{aligned} \tag{8}$$

The requirements of the closed-loop system with feedforward control need to meet a phase margin larger than 35 deg of the open-loop transfer function, we have

$$\arg[S_{\text{open}}(s)|_{s=jw_c'}]+180\,\text{deg}\geq 35. \tag{9}$$

The feedforward control is expected to have little influence on the closed-loop BW, resulting in $w_c'\approx w_c$. Substituting the results of the PI controller parameters into Eq. (8), we get $T_f\geq 1.893T_0$, from which it can be deduced

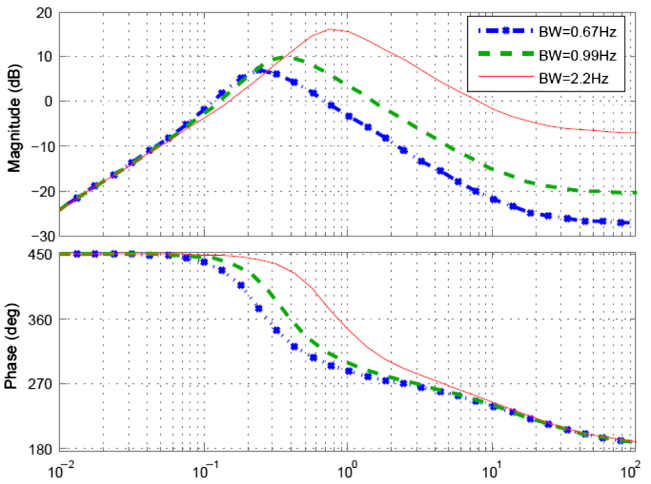

Fig. 4 Velocity response based Kalman filter.

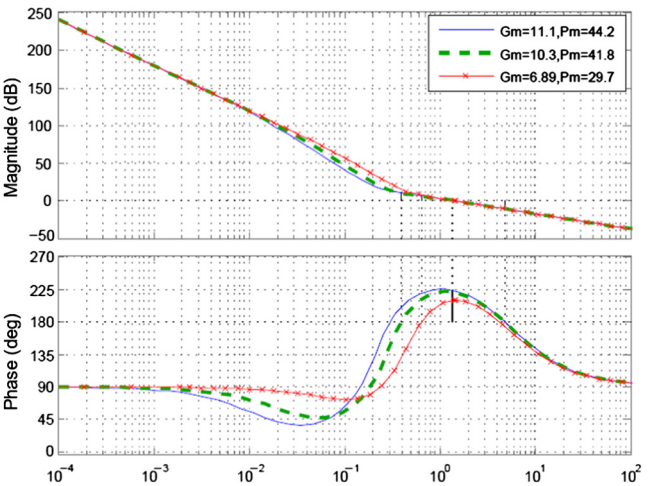

Fig. 5 The open-loop response while the process variance of the Kalman filter is varying.

that the BW of the filter must be limited to less than $1/(1.893T_0) = 1.221$ Hz.

The Kalman filter is an optimal linear mean minimum square filter to suppress noise. The target velocity can be estimated by the Kalman filter and be fed into the control system. The standard Kalman equations are depicted as follows:

$$\begin{cases} x_{k+1} = Ax_k + Bu + w_k \\ y_{k+1} = Cx_k + v_k \end{cases}. \tag{10}$$

The observed signal is the target trajectory recovered by LOS error and the angular position. A simple mode called the Singer acceleration model, nicknamed the zero-mean first-order Markov model,[9] is used to estimate the target speed. Then we can easily know the Kalman filter parameters as follows:

$$\begin{aligned} A &= \begin{bmatrix} 1 & T & 0.5T^2 \\ 0 & 1 & T \\ 0 & 0 & 1 \end{bmatrix}, \\ B &= \begin{bmatrix} \frac{1}{6}T^3 & \frac{1}{2}T^2 & T \end{bmatrix}^T, \\ C &= \begin{bmatrix} 1 & 0 & 0 \end{bmatrix}. \end{aligned} \tag{11}$$

The solution of the Kalman filter is given below:

$$\hat{x}_{k+1} = (A - K_{k+1}CA)\hat{x}_k + K_{k+1}y_k. \tag{12}$$

The gain K_{k+1} of the Kalman filter can be obtained from the Ricatti equation if the matrices A, B, and C are time invariant. Using the "dare" function can help to quickly solve the Ricatti equation. The reconstructive characteristics of the Kalman filter in the frequency domain can be described in Eq. (13):

$$\varphi = (ZI - A + K_{k+1}CA)^{-1}K_{k+1}. \tag{13}$$

The bode plot indicates that the target speed is pretty efficient in low frequencies in Fig. 4, where the phase lags a little. The bigger the process variance is, the higher the BW of the Kalman filter. A high BW probably leads to control system instability, although it has enough margin to adapt to a maneuvering target.

The BW of the Kalman filter needs to be smaller than 1.2 Hz according to the analysis above. The green line in Fig. 4 illustrates the Kalman filter response for which the BW is about 0.99 Hz.

4 Stability and Improvement Analysis

From the sensitivity transfer function, the misalignment of two kinds of time parameters and the BW of the Kalman filter jointly affect the closed loop stability. The open-loop transfer function responses in Fig. 5 correspond to the different BWs of the Kalman filter in Fig. 4. A high BW of the Kalman filter weakens the margin of the open-loop control system and even leads to instability. In this paper, the Kalamn filter with a BW of 0.99 Hz is preferable in this control system, while the phase margin (Pm) and the gain margin (Gm) of the open-loop transfer function [Eq. (4)] are 41.8 deg and 10.3 dB, respectively. The sensitivity function without a feedforward control is as follows:

$$S'_{\mathrm{SF}} = \frac{e^{-T_0 s}}{1 + C(s)P(s)e^{-T_0 s}}. \tag{14}$$

Based on these considerations and design, the responses in the sensitivity function [Eqs. (1) and (14)] are shown in Fig. 6. A large attenuation, about one-tenth less than that with only a feedback loop control, is achieved in the low-frequency region with a feedforward controller in Fig. 6. However, the attenuation in the middle-frequency range is magnified from 0.2 Hz to about 0.4 Hz, a little larger than that with only the feedback control. This is due to the amplification by the Kalman filter.

It is natural that the misalignment error inevitably occurs, although the sample frequency of the encoder can reach several thousand hertz or more while the CCD has usually a few dozens of hertz. In comparison with the Kalman filter, we can see from Fig. 7 that the deviations of the misalignment between the two parameters have little effect on the stability.

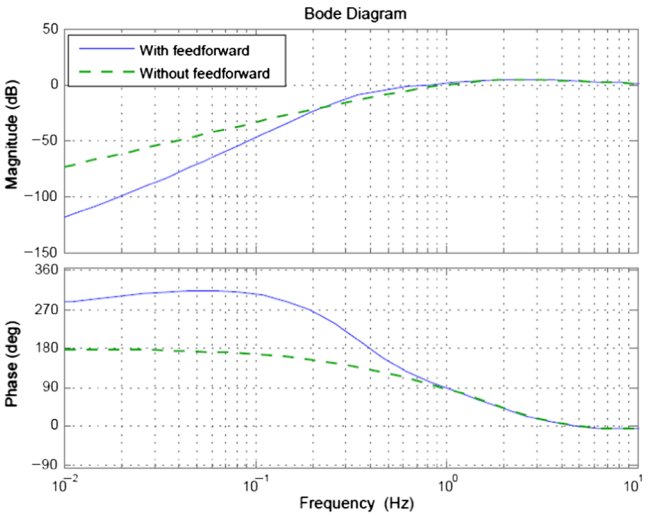

Fig. 6 The sensitivity function response.

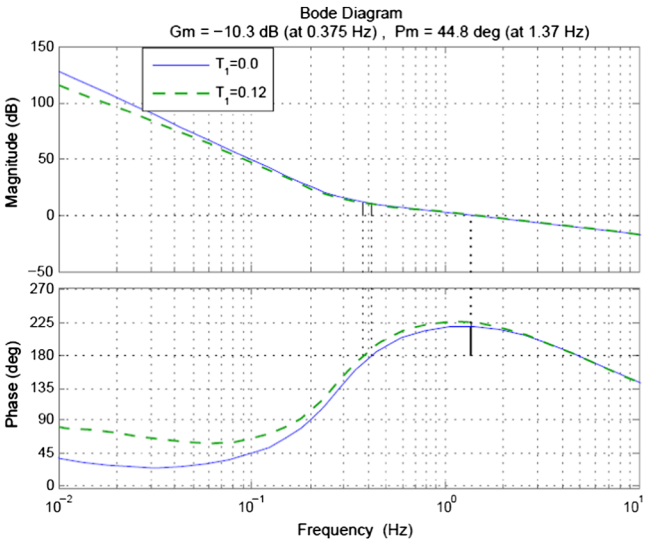

Fig. 7 The open-loop response while the time delay is varying.

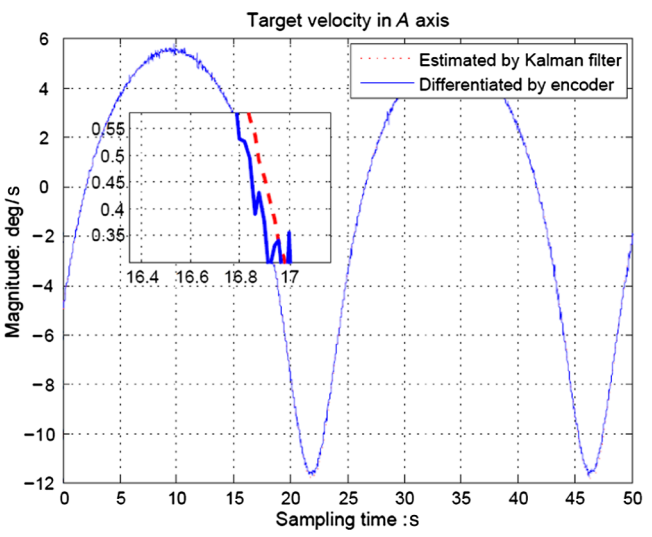

Fig. 8 The target speed in the *A* axis.

5 Experimental Setup

The trajectory of a moving target is provided by dynamic moving target simulators. A two-axis gimbal with a 50-Hz CCD as a tracker is used to track the moving target, for which the angular speed differentiated by a position angular from encoder is about 11.8 deg /s for the azimuth axis and 5 deg /s for the elevation axis in Figs. 8 and 9. The target acceleration is obtained by further differentiating the speed, about 4 deg /s^2 for the azimuth axis and 2 deg /s^2 for the elevation axis in Fig. 10.

Comparing the target velocity estimated with the Kalman filter with the target velocity by the differentiating encoder, the noise is suppressed by the Kalman filter.

In Fig. 11, A stands for the azimuth axis, whereas E represents the elevation axis. The LOS error with the feedforward control is shown in Fig. 11, and is much less than that without a feedforward control whose error curve is not drawn because the field of view of this CCD is too narrow to accommodate the 0.2-deg range.

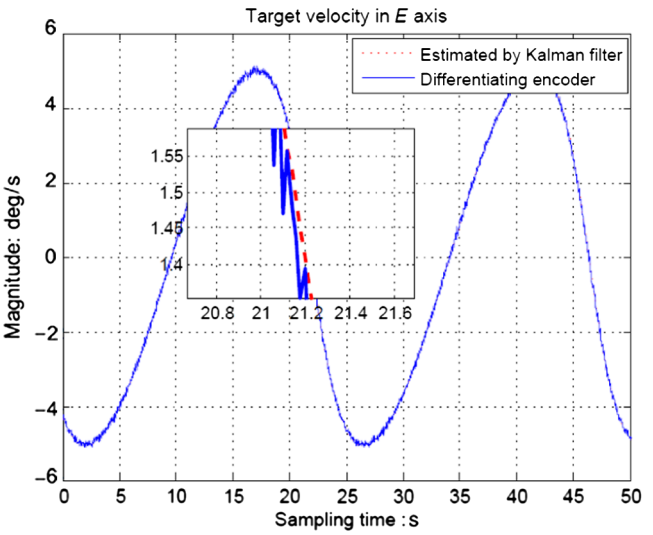

Fig. 9 The target speed in the *E* axis.

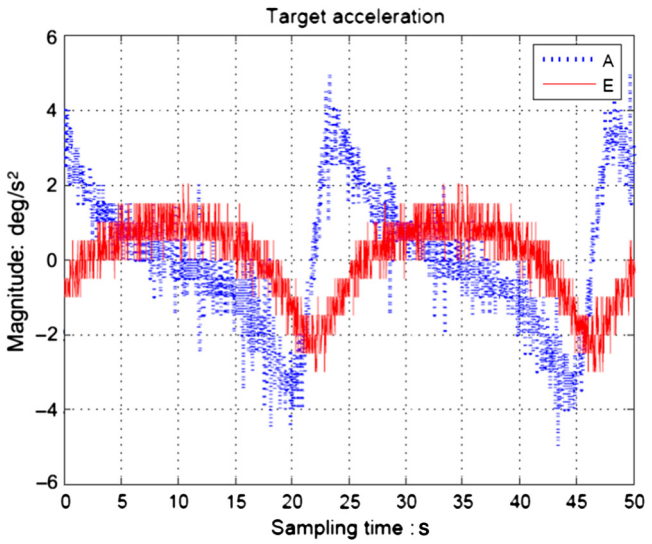

Fig. 10 The target acceleration.

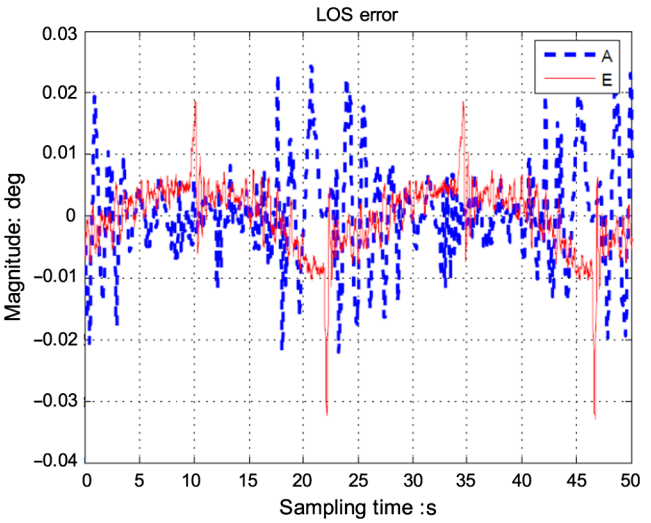

Fig. 11 The line-of-sight (LOS) error.

6 Conclusions

This paper—focusing on the implementation of the feedforward control, the optimization of the control parameters, and the detailed stability analysis—proposes a feedforward control mechanism and configuration based on data fusion in a CCD-based tracking system. Experiments verify that this technique effectively enhances the closed-loop performance in comparison with the classical control mode. Related topics not covered in this paper are how to optimize the control parameters in an all-around manner rather than in an independent way and what kind of filters must be used to estimate target speeds and their effects on control stability. Furthermore, it is very challenging to investigate acceleration feedforward[12] to improve performance further.

Acknowledgments

The authors thank anonymous reviewers for their valuable comments, and also give thanks to the Youth Innovation Promotion Association, Chinese Academy of Science, and the China scholarship council for their sponsorship.

References

1. S. Hutchinson, G. D. Hager, and P. I. Corke, "A tutorial on visual servo control," *IEEE Trans. Rob. Autom.* **12**(5), 651–670 (1996).
2. B. L. Ulich, "Overview of acquisition, tracking, and pointing system technologies," *Proc. SPIE* **887**, 40–63 (1988).
3. P. I. Corke, *Visual Control of Robots: High-Performance Visual Servoing*, Robotics and Mechatronics Series, 2, Research Studies Press (John Wiley), Taunton, England (1996).
4. B. Ekstrand, "Tracking filters and models for seeker applications," *IEEE Trans. Aerosp. Electron. Syst.* **37**(3), 965–976 (2001).
5. J. M. Fitts, "Aided tracking as applied to high accuracy pointing systems," *IEEE Trans. Aerosp. Electron. Syst.* **9**(3), 350–368 (1973).
6. M. Tomizuka, "Control methodologies for manufacturing applications," *Manuf. Lett.* **1**(1), 46–48 (2013).
7. X. Chen and M. Tomizuka, "New repetitive control with improved steady-state performance and accelerated transient," *IEEE Trans. Control Syst. Technol.* **22**(2), 664–675 (2014).
8. D. Tenne and T. Singh, "Tracking for maneuvering target trajectories via the 3D circular filter," *IEEE Trans. Aerosp. Electron. Syst.* **23**(3), 298–310 (1987).
9. X. R. Li and V. P. Jilkov, "A survey of maneuvering target tracking: dynamic models," *Proc. SPIE* **4048**, 212–236 (2000).
10. B. J. Lee, Y. H. Joo, and J. B. Park, "An intelligent tracking method for a maneuvering target," *Int. J. Control Autom. Syst.* **1**(1), 93–100 (2003).
11. R. Horowitz et al., "Dual-stage servo systems and vibration compensation in computer hard disk drives," *Control Eng. Pract.* **15**(3), 291–305 (2007).
12. M. Boerlage et al., "Model based feedforward for motion systems," in *Proc. IEEE Conf. Control Applications*, Vol. 2, pp. 1158–1163, Istanbul, Turkey (2003).

Tao Tang received his PhD in 2009 from the Institute of Optics and Electronics, Chinese Academy of Sciences. He joined this institute after his graduation, where he is currently an associate professor. His research interests include control-based sensors, FSM control, adaptive control, and inertial stabilization.

Huaxiang Cai is a PhD candidate in the Institute of Optics and Electronics, Chinese Academy of Sciences. His research interests include control-based sensors, FSM control, adaptive control, and tracking control.

Yongmei Huang is with the Institute of Optics and Electronics, Chinese Academy of Sciences. She received her doctoral degree in 2004, and now is a professor and doctor director in the Institute of Optics and Electronics. Currently, her research interests include technology of beam control and optical engineering.

Ge Ren is with the Institute of Optics and Electronics. He is a professor and doctor director in the Institute of Optics and Electronics. Currently, his research interests include technology of beam control and optical engineering.